



Stellar Loci. VII. Photometric Metallicities of 5 Million FGK Stars Based on GALEX GR6+7 AIS and Gaia EDR3

3-22

arxiv:2311.16901v2

Reporter: Baokun Sun

Outline

- 1. Introduction
- 2. Data
- 3. Method
- 4. Results and Discussion
- 5. The final sample
- 6. Summary

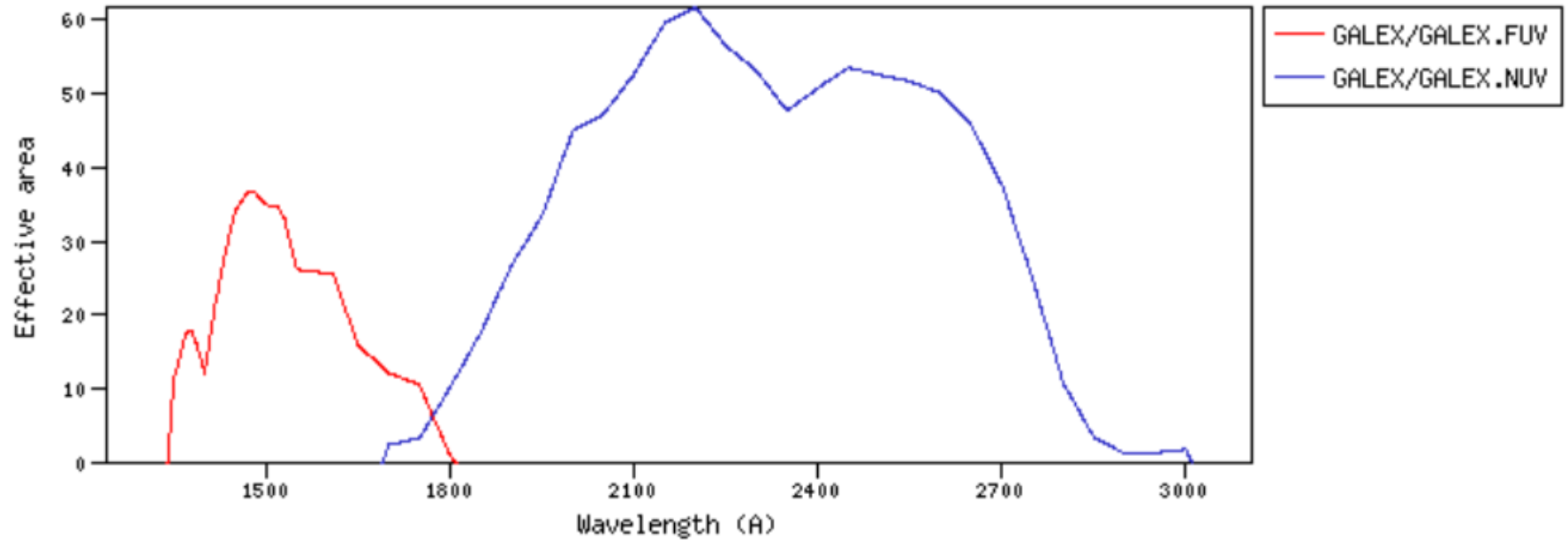
Introduction

- Metallicity is one of the basic stellar parameters, and plays an important role in studying **the formation and evolution** of not only stars and stellar populations, but also of galaxies such as the Milky Way.
- There are two main methods to estimate stellar metallicity for large samples of stars utilized to date: **spectroscopic and photometric**.
- Spectroscopic surveys are more **time-consuming** and require **complex data analysis** compared to photometric surveys. The resulting limited samples, coupled with typically **complex selection functions** for the targets.

Introduction

- A typical procedure for obtaining photometric metallicity estimates involves several steps. First, cross-matches of photometric catalogs of stars with available spectroscopic-metallicity estimates are performed.
- **Data quality cuts** and careful **reddening corrections** are then applied for the stars in common.
- Subsequently, various techniques such as metallicity-dependent stellar loci fitting.
- Finally, the established relationship is applied to all photometric data that satisfy certain conditions, enabling the determination of photometric metallicities for those sources.

- GALEX use of near-UV



- Most stars

- The unpr

	# sources in Gaia EDR3
Total number of sources	1,811,709,771
Number of 5-parameter sources	585,416,709
Number of 6-parameter sources	882,328,109
Number of 2-parameter sources	343,964,953
Sources with mean G magnitude	1,806,254,432
Sources with mean G_{BP} -band photometry	1,542,033,472
Sources with mean G_{RP} -band photometry	1,554,997,939
Gaia-CRF sources	1,614,173
Sources with radial velocities	7,209,831 (Gaia DR2)
Variable sources	expected with Gaia DR3 / see Gaia DR2
Known asteroids with epoch data	expected with Gaia DR3 / see Gaia DR2
Effective temperatures (T_{eff})	expected with Gaia DR3 / see Gaia DR2
Extinction (A_G) and reddening ($E(G_{BP}-G_{RP})$)	expected with Gaia DR3 / see Gaia DR2
Sources with radius and luminosity	expected with Gaia DR3 / see Gaia DR2
and more...	expected with Gaia DR3

h

ides
for

Construction of Training Samples

- $0.4 < (BP - RP)_0 < 1.6$ for dwarfs and $0.6 < (BP - RP)_0 < 1.6$ for giants.
- $NUV > 15$ to avoid saturation (Morrissey et al. 2007) and $errorNUV < 0.1$ to ensure the NUV data quality.
- $-3.5 < [Fe/H] < +0.5$ for dwarfs (considering the metallicity dependency is too weak to estimate metallicity for dwarf stars with $[Fe/H] < -3.5$ using the GALEX NUV data) and $-5 < [Fe/H] < +0.5$ for giants.
- $phot_bp_rp_excess\ factor < 0.09 \times (BP - RP) + 1.15$ to ensure the BP/RP data quality.
- $E(B - V) < 0.15$. The $E(B - V)$ used here is from the Schlegel et al. (1998, hereafter **SFD98**) dust reddening map.

Construction of Training Samples

- Finally, a total of 1073 and 1107 sources are selected as our dwarf and giant training samples, respectively.

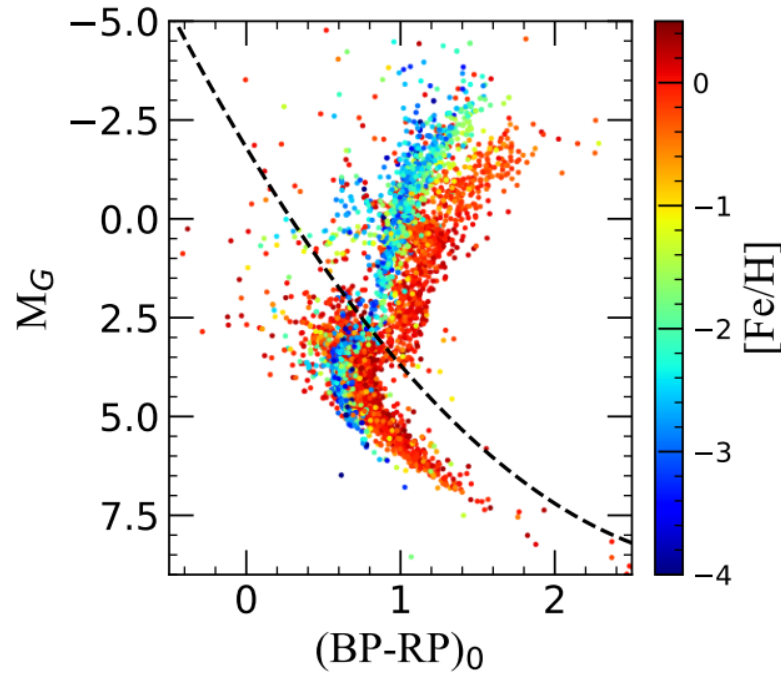


Figure 1. H-R diagram of the training samples, color-coded by $[Fe/H]$. The dwarfs and giants are separated by the black-dashed line (Xu et al. 2022a): $M_G = -(BP - RP)^2 + 6.5 \times (BP - RP) - 1.8$.

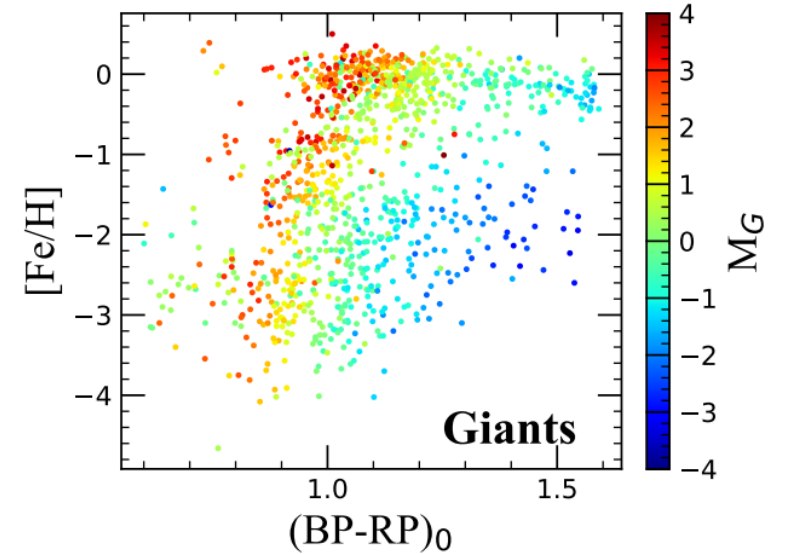
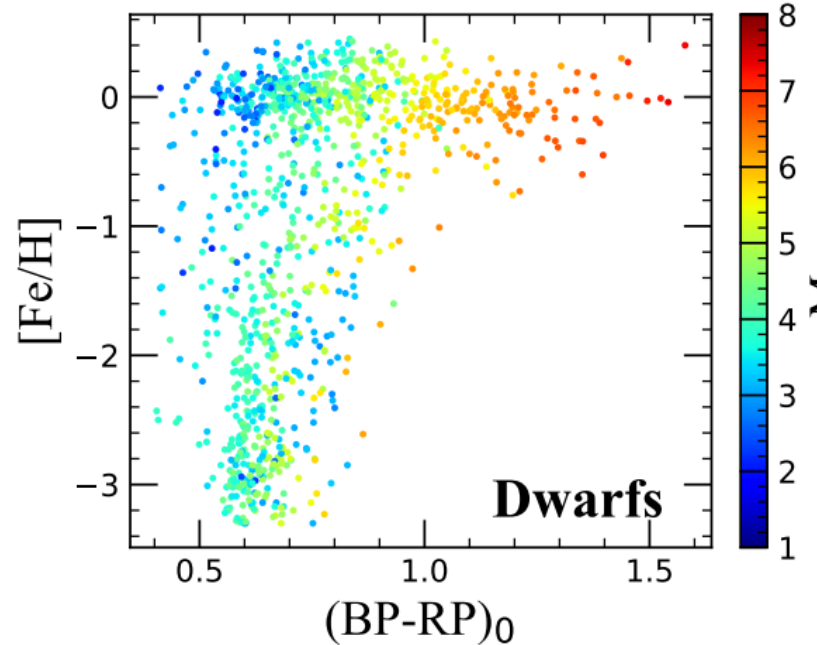
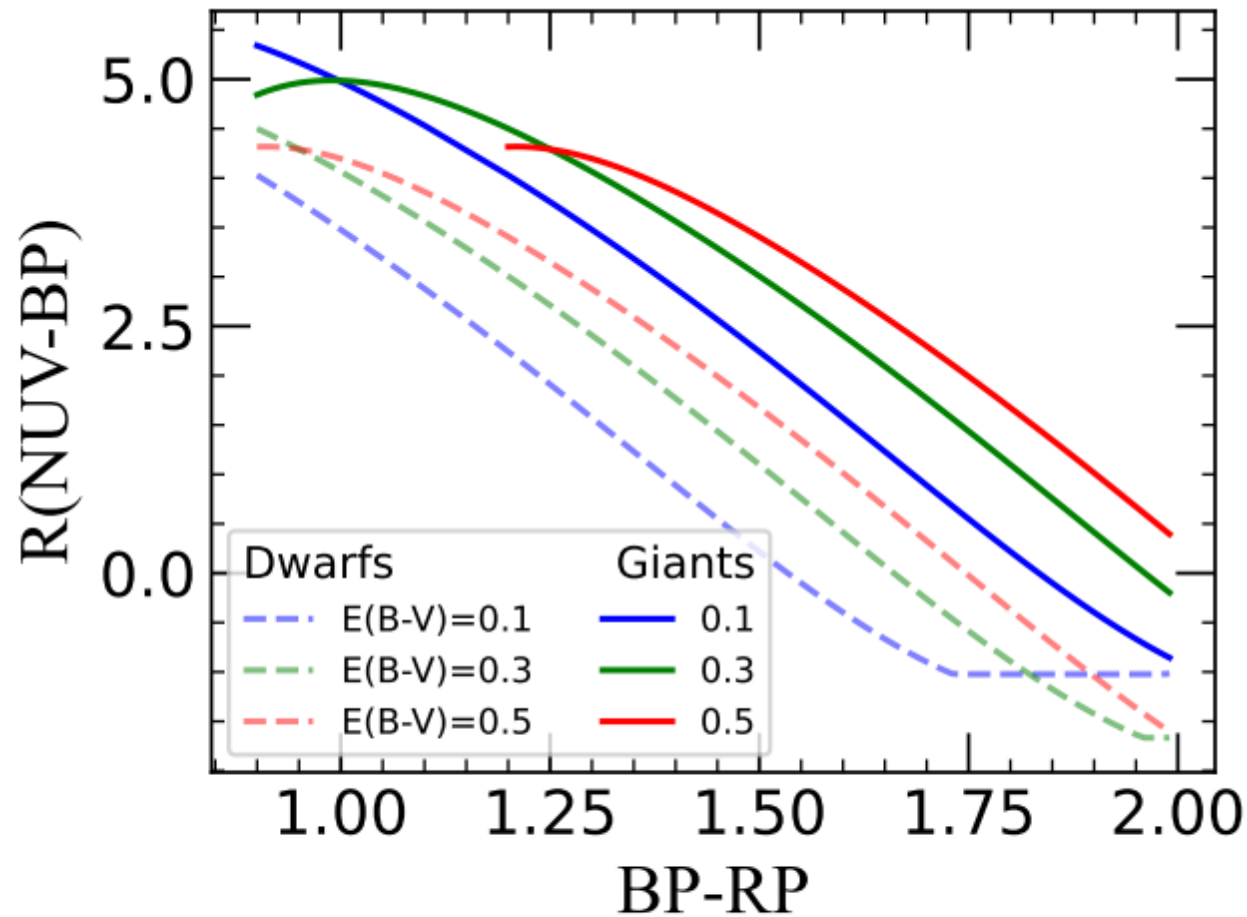


Figure 2. Distributions of the dwarf (top panel) and giant (bottom panel) training samples after cutting in the $[Fe/H]$ vs. $(BP - RP)_0$ plane, color-coded by M_G .

- Due to the careful reddening
- Zhang & Yu: coefficients empirical re



perform
ing
option of
d coefficients.

Figure 4. $R_{\text{NUV-BP}}$, as a function of BP-RP , for dwarfs (dashed lines) and giants (solid lines) at different extinction values.

[Fe/H]- and MG-dependent Stellar Loci

- Similar to Yuan et al. (2015a), we conduct a polynomial fitting for stellar loci, and employ a minimum χ^2 technique to derive the metallicity for dwarfs and giants, respectively.

where X , Y , Z represents the BP–RP color, [Fe/H], and MG, respectively.

$$\begin{aligned} (NUV - BP) = & \\ & p0 \cdot X^4 + p1 \cdot Y^4 + p2 \cdot Z^4 + p3 \cdot X^3 \cdot Y \\ & + p4 \cdot Y^3 \cdot X + p5 \cdot X^3 \cdot Z + p6 \cdot Z^3 \cdot X \\ & + p7 \cdot Z^3 \cdot Y + p8 \cdot Y^3 \cdot Z + p9 \cdot X^2 \cdot Y^2 \\ & + p10 \cdot X^2 \cdot Z^2 + p11 \cdot Z^2 \cdot Y^2 + p12 \cdot X^3 \\ & + p13 \cdot Y^3 + p14 \cdot Z^3 + p15 \cdot X^2 \cdot Y + p16 \cdot Y^2 \cdot X \\ & + p17 \cdot X^2 \cdot Z + p18 \cdot Z^2 \cdot X + p19 \cdot Z^2 \cdot Y \\ & + p20 \cdot Y^2 \cdot Z + p21 \cdot X^2 + p22 \cdot Y^2 + p23 \cdot Z^2 \\ & + p24 \cdot X \cdot Y + p25 \cdot Y \cdot Z + p26 \cdot X \cdot Z \\ & + p27 \cdot X + p28 \cdot Y + p29 \cdot Z + p30, \end{aligned} \quad (1)$$

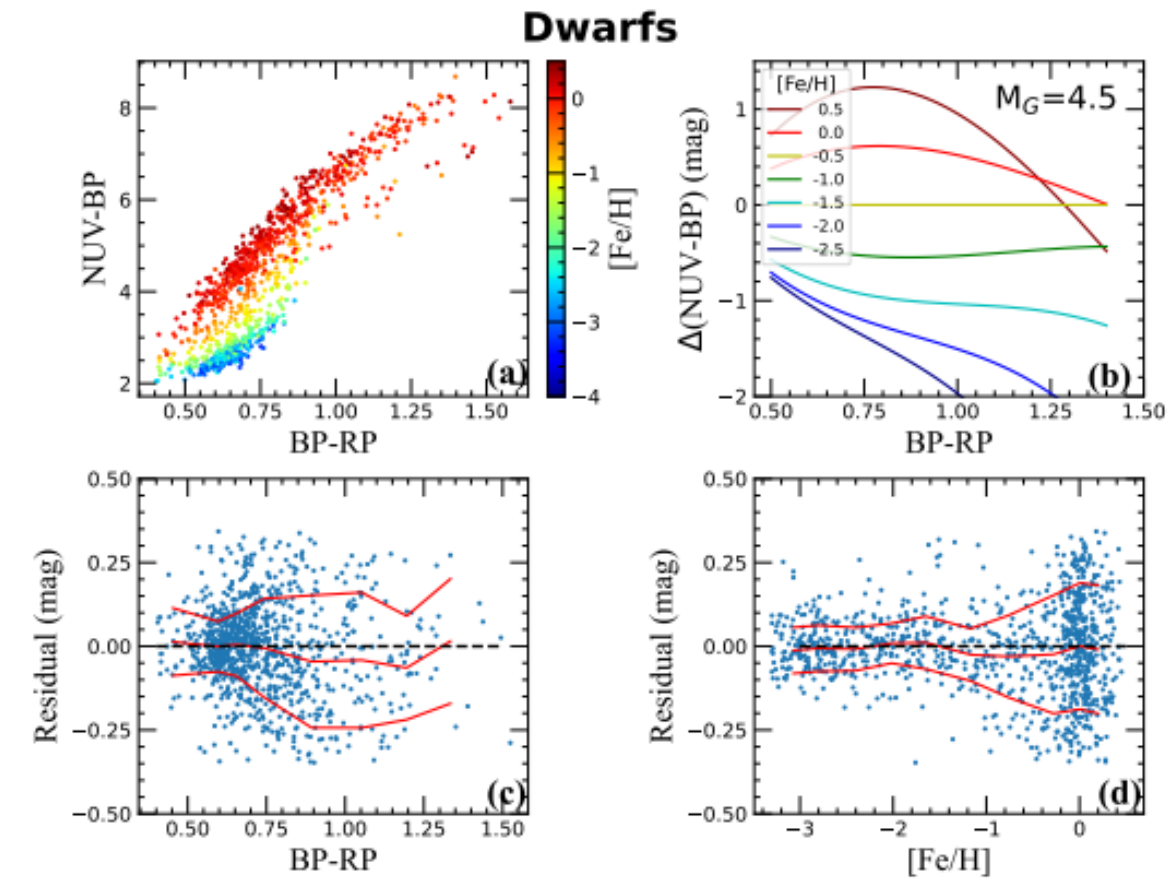


Figure 5. Panel (a): Distributions of the dwarf training sample in the NUV-BP vs. BP-RP plane (stellar loci), color-coded by [Fe/H] as shown in the right color bar. Panel (b): When $M_G = 4.5$, the variations of stellar loci for different metallicities (as shown in the label) relative to the one at [Fe/H] = -0.5. Panels (c-g): Fitting residuals as a function of BP-RP color, [Fe/H], M_G , $E(B-V)$, and NUV, respectively. The red-solid lines indicate the median values and standard deviations. The black-dashed line indicates the zero level. Panel (h): Histogram distribution of the fitting residuals, with the Gaussian fitting profile over-plotted in black.

External Tests with LAMOST DR8

Due to the over-estimation of extinction values in the SFD98 reddening map close to the Galactic plane, there is an over-estimation of $[\text{Fe}/\text{H}]$ in our model for the stars in this region, as shown in the top row of panels (especially in dwarfs).

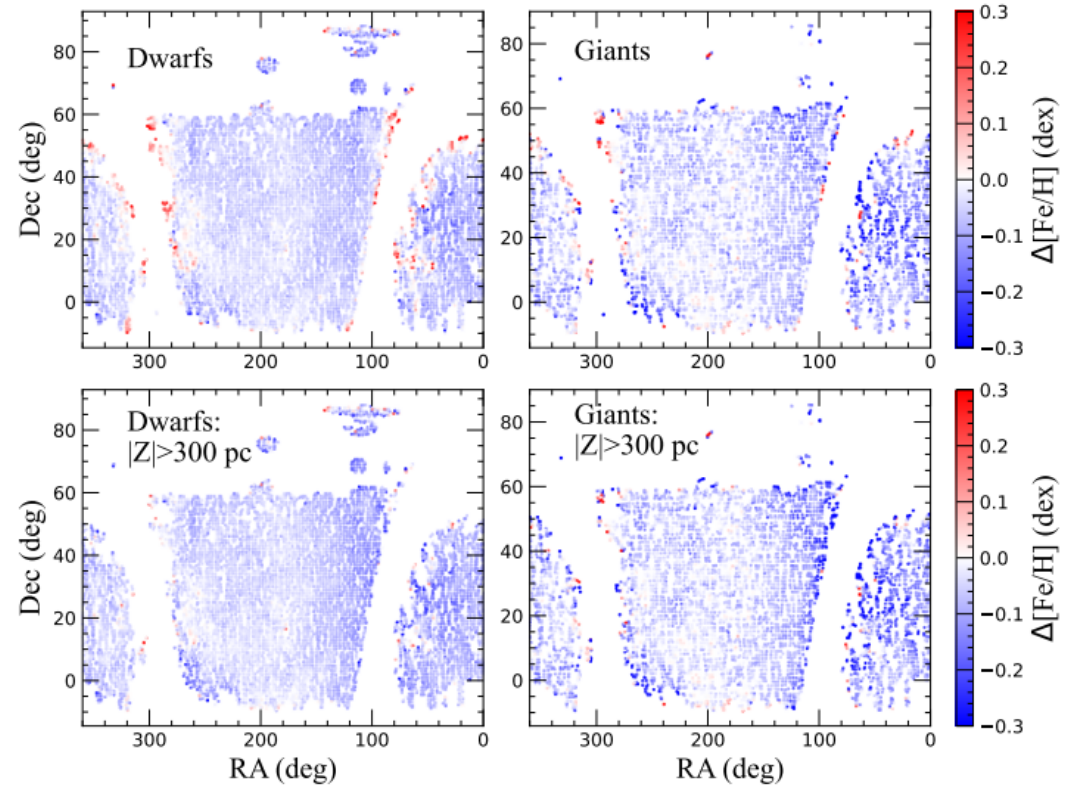


Figure 11. The spatial distribution (RA and Dec) of the residuals $\Delta[\text{Fe}/\text{H}]$. The top row of panels are for the test-with-LAMOST sample of 633,807 dwarfs and 72,911 giants, respectively. The bottom row of panels are the sub-sample of these stars with $|Z| > 300$ pc (441,141 dwarfs and 64,696 giants, respectively.)

Thus, between the over-estimates or under-estimates of NUV–BP colors caused by photometric errors, the under-estimates lead to a larger under-estimation in the calculation of photometric metallicities.

Overall, from these tests, $[\text{Fe}/\text{H}]$ estimates from our model are reliable even for metallicity down to $[\text{Fe}/\text{H}] \sim -3.5$.

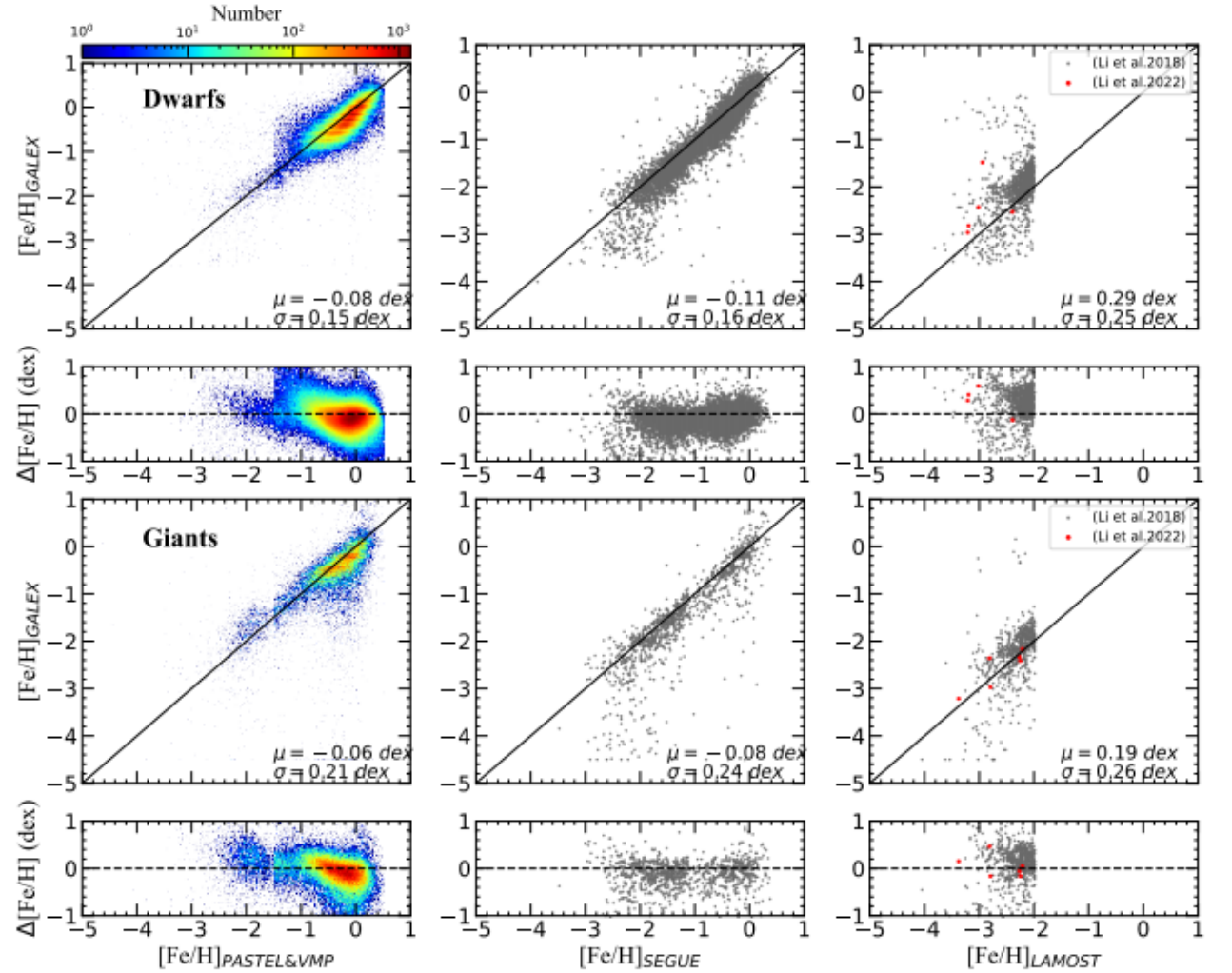


Figure 12. From left to right, the columns of panels represent comparisons with the LAMOST DR8 value-added catalog of Wang et al. (2022), the SEGUE DR12 (Alam et al. 2015) catalog, and the VMP catalogs of Li et al. (2018) and Li et al. (2022), respectively. The left column of panels is color-coded by the source number density. In the right column of panels, the gray and red dots are from Li et al. (2018) and Li et al. (2022), respectively. The dwarfs are plotted in the top row of panels and the giants in the bottom row of panels. The mean and standard deviation values of the residuals $\Delta[\text{Fe}/\text{H}]$ are labeled in the lower-right of each panel.

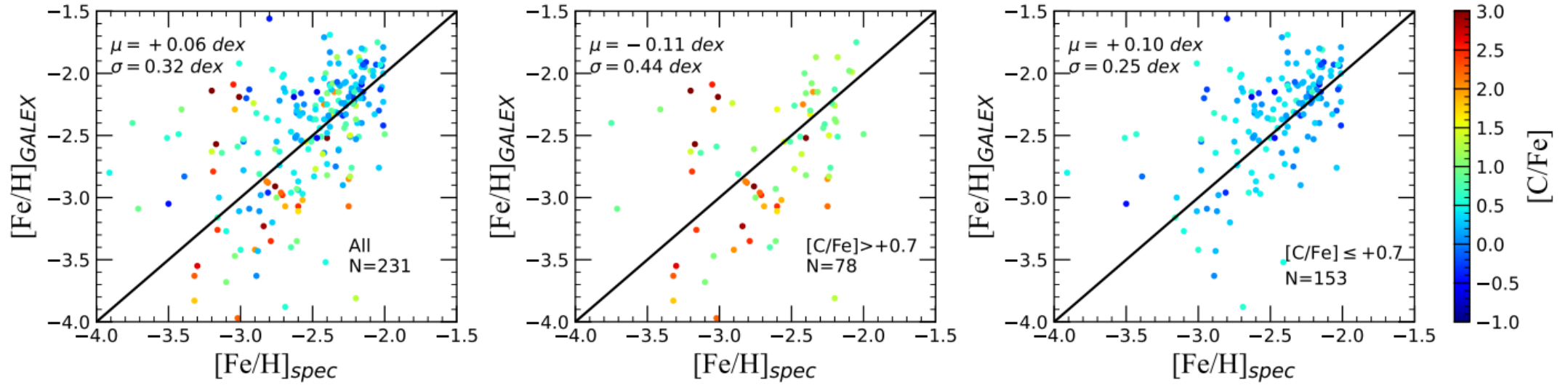


Figure 14. Comparisons of $[\text{Fe}/\text{H}]_{\text{GALEX}}$ with spectroscopic measurements for VMP/EMP stars (taken from the compilation of Hong et al. 2023), color-coded by $[\text{C}/\text{Fe}]$. From left to right, the panels show the full sample, the sub-sample of stars with $[\text{C}/\text{Fe}] > +0.7$, and the sub-sample of stars with $[\text{C}/\text{Fe}] \leq +0.7$, respectively. The mean and standard deviation values of the residuals $\Delta[\text{Fe}/\text{H}]$ are labeled in the upper-left of each panel. Note that, in all three panels, there are stars with $[\text{Fe}/\text{H}]_{\text{GALEX}}$ that straddle the black-solid one-to-one lines; they are *not* uniformly biased high due to the effect of carbon, as has been seen to occur for several previous photometric-metallicity techniques (see text).

- 1) the fact that the sub-sample of stars with $[\text{C}/\text{Fe}] > +0.7$ are bluer (and less sensitive to $[\text{Fe}/\text{H}]$) and fainter (larger photometric errors), and thus have larger uncertainties in the $[\text{Fe}/\text{H}]_{\text{GALEX}}$ estimates and,
- 2) the effects of carbon enhancement on our estimates, primarily for the cooler giants in our sample.

Summary

- In this work, we combine the SAGA and PASTEL catalogs with Gaia EDR3 and GALEX GR6+7 AIS data as our training sample to construct a relational model from stellar loci that incorporate MG to estimate photometric metallicities for dwarfs and giants.
- They have obtained a typical precision of **0.11 dex** for dwarfs and **0.17 dex** for giants, with an effective metallicity range from $-3.0 < [\text{Fe}/\text{H}] \leq +0.5$ for dwarfs and $-4.0 < [\text{Fe}/\text{H}] \leq +0.5$ for giants.
- Their measurements could be used to provide a more complete census of VMP and EMP stars, and to select C-enhanced VMP stars and N-enhanced stars